Supporting Information

Liang et al. 10.1073/pnas.1302825110

SI Materials and Methods

Cell Culture and Treatment. The immortalized human mammary epithelial cell (HMLE)-Twist-ER which were generously provided by R. Weinberg (Whitehead Institute for Biomedical Research, Massachusetts Institute of Technology, Cambridge, MA), were generated by infecting the HMLE cells with tamoxifen inducible pWZL-Twist-ER vectors followed by selection with 5 ng/mL of blasticidin and maintained in serum-free MEGM with supplements and growth factors (CC-3150; Lonza). For epithelial–mesenchymal transition (EMT) induction, HMLE-Twist-ER cells were exposed to 4-hydroxytamoxifen (Sigma) at 20 nM for 12 d as described (1). Human breast cancer cell lines MCF-7 were obtained from the American Type Culture Collection and cultured in DMEM (high glucose) containing 10% (vol/vol) FBS and Roswell Park Memorial Institute medium containing 10% (vol/vol) FBS, respectively.

Flow Cytometry. Cells were detached with trypsin/EDTA and single cells were washed with PBS containing 2% (vol/vol) FBS. For single-color fluorescence staining, cells were incubated with the indicated primary antibodies for 10 min. After washing, the cells were incubated with appropriate secondary antibodies conjugated with phycoerythrin (PE) (Beckman Coulter) for 20 min. For triple-color fluorescence staining, cells were first stained with anti-glycosphingolipid (GSL) antibodies or isotype controls. Next, cells were stained with PerCPcy5.5-anti-CD44 and ECD-anti-CD24. Approximately 1×10^6 cells were stained, and 1×10^5 events were analyzed with an LSR II flow cytometer (BD Biosciences) and FlowJo software.

Mammosphere Assay. MCF-7 cells (2×10^3) were plated in ultra-low-attachment 24-well dishes (Costar) in serum-free Mammary Epithelial Cell Growth Medium (MEGM) basal medium supplemented with all required growth factors as described in *Materials and Methods* in the main text for the growth of HMLE-Twist-ER cells, except bovine pituitary extract with B-27 supplements (1×, Invitrogen). After 5 d of culture at 37 °C, resulting mammospheres were counted under microscope.

Antibodies. Anti-Gb3 mAb 1A4 was created in our laboratory (2). Anti-GM2 mAb MK1-8 (3) was kindly provided by Reiji Kannagi (Institute of Biomedical Sciences, Academia Sinica, Taipei, Taiwan). The other antibodies were obtained as follows: anti-GD2 mAb 14.G2a, PerCPcy5.5-anti-CD44, and ECD-anti-CD24 (BD Pharmingen); anti-GD3 (mAb clone R24; Abcam); anti-GD1a (mAb clone GD1a-1; Millipore); and PE-goat-anti-mouse-IgG, PE-goat-anti-mouse-IgM, and isotype controls (Beckman Coulter).

Real-Time RT-PCR. Total RNA was extracted and purified using an RNeasy Plus Mini Kit (Qiagen). The first strand of cDNA was prepared from 5 μg of RNA using SuperScript III first-strand Synthesis SuperMix (Invitrogen) with random primers, according to the manufacturer's instructions. RT-PCR was performed using Applied Biosystems StepOnePlus system according to the manufacturer's protocol. Two hundred nanograms of cDNA was used and relative quantities of mRNAs were determined using the comparative threshold number (Ct value) method. β-actin and Ups11 were used as reference genes.

Gold Colloidal Phagokinetic Track Assay for Cell Motility. Gold sol-coated plates (24-well) were prepared as described previously (4, 5). Cells were detached with trypsin/EDTA and 5×10^2 cells in complete culture medium were seeded onto gold sol-coated wells and incubated for 18 h. Photos were taken, and track areas for 30 cells were measured using the ImageJ program and expressed in square pixels.

GSL Extraction, High-Performance TLC Analysis, and Immunostaining. GSL extraction was performed as described previously (6). Cells (2×10^8) were extracted by sonication four times in 10 mL of each of the following solvents in succession: (*i*) chloroform/methanol (1:1), (*ii*) isopropanol/hexane/water (55:25:20, lower phase), (*iii*) isopropanol/hexane/water (55:25:20, lower phase), and (*iv*) chloroform/methanol (1:1). The combined extracts were evaporated and dissolved in 6 mL of chloroform/methanol (2:1). The solution was added to 1 mL of water to achieve chloroform:methanol:water (CMW) 4:2:1 then shaken and allowed to separate into upper and lower phases. The lower phase was added to 3 mL of chloroform/methanol/0.1% NaCl (1:10:10), shaken, and allowed to separate into upper and lower phases (this step, Folch partition, was repeated three times). Upper phases were combined and washed once with 0.5 mL of chloroform/methanol (2:1). The upper phase was evaporated and solubilized in distilled water and the resultant solution was applied to a Sep-Pak C18 cartridge (Varian) for desalting.

The Folch partition lower phase was further purified by acetylating methods to remove phospholipids as described previously (6). The lower phase was completely dried and acetylated by 1 mL of dried pyridine and 0.5 mL of acetic anhydride for 16–18 h. Acetylated GSLs were evaporated and dissolved in hexane-dicyanoethylene (DCE) 1:4. The peracetylated GSLs was passed through a Florisil column and washed by hexane-DCE 1:4. After washing, the column was eluted with DCE or DCE-acetone 1:1. Only the eluent with DCE-acetone 1:1 was collected and evaporated to dryness; this eluent contained glycolipids purified from total phospholipids. Acetylated glycolipids were next dissolved in 0.2 mL of methanol and then deacetylated by adding 0.1 mL of 2.5% (wt/vol) sodium methoxide (Sigma). After 3 h, the mixture was neutralized with ethyl acetate. Total reaction mixtures were evaporated to dryness under N_2 stream, dissolved in water, and then desalted by Sep-Pak C18 cartridge (Varian).

GSLs from the Folch partition upper or lower phases were eluted with chloroform/methanol (2:1) from Sep-Pak C18 cartridges, analyzed using high-performance TLC (HPTLC) plates (EMD Bioscience), developed in a solvent system of chloroform/methanol/0.5% aqueous $CaCl_2$ (50:40:10), and visualized by spraying with 0.5% orcinol in 1 M sulfuric acid.

GSLs from the Folch partition upper phase were class-separated as described (7). GSLs were dissolved in CMW (30:60:8), loaded on a DEAE Sephadex column, and eluted with CMW (30:60:8) to obtain neutral GSLs. The column was eluted successively with CMW (30:60:8) containing ammonium acetate at the following concentrations: (*i*) 0.03 M to obtain monosialo-gangliosides, (*ii*) 0.13 M to obtain disialo-gangliosides, (*iii*) 0.45 M to obtain trisialo-gangliosides, and (*iv*) 0.8 M to obtain polysialo-gangliosides. Each eluent was dried, dialyzed, and then analyzed by HPTLC as above.

GSLs were further analyzed by HPTLC immunostaining, as previously described (8). GSLs were developed on HPTLC plates and the plates were dried, fixed with 5% (wt/vol) poly (isobutylmetacrylate) in hexane/chloroform (9:1), blocked with 3% (wt/vol) BSA in PBS, and incubated with mAbs directed to various GSLs. TLC plates were then incubated with appropriate secondary antibodies conjugated to horseradish peroxidase and were detected by chemiluminescence detection kit (Pierce).

Immunofluorescence Cell Staining. For cell-surface GSL staining, cells were fixed in 4% (wt/vol) formaldehyde in PBS for 30 min. After washing, cells were blocked in PBS containing 10% (vol/vol) FBS and 1% (wt/vol) BSA then incubated with appropriate concentrations of the primary antibody and then with Alexa-594–conjugated secondary antibody in blocking solution. Subsequently, cells were stained with Hoechst 33258 (Invitrogen)/PBS for 1 min. A coverslip was mounted with glycergel mounting medium (Dako) and sealed with clear nail polish. Fluorescent images were observed under a Zeiss confocal immunofluorescence microscope.

1. Mani SA, et al. (2008) The epithelial-mesenchymal transition generates cells with properties of stem cells. *Cell* 133(4):704–715.
2. Kojima H, Tsuchiya S, Sekiguchi K, Gelinas R, Hakomori SI (1987) Predefined gene transfer for expression of a glycosphingolipid antigen by transfection with a cosmid genomic library prepared from a cell line in which the specific glycosphingolipid is highly expressed. *Biochem Biophys Res Commun* 143(2):716–722.
3. Miyake M, et al. (1988) Generation of two murine monoclonal antibodies that can discriminate N-glycolyl and N-acetyl neuraminic acid residues of GM2 gangliosides. *Cancer Res* 48(21):6154–6160.
4. Mitsuzuka K, Handa K, Satoh M, Arai Y, Hakomori SI (2005) A specific microdomain ("glycosynapse 3") controls phenotypic conversion and reversion of bladder cancer cells through GM3-mediated interaction of alpha3beta1 integrin with CD9. *J Biol Chem* 280(42):35545–35553.
5. Todeschini AR, Dos Santos JN, Handa K, Hakomori SI (2007) Ganglioside GM2-tetraspanin CD82 complex inhibits met and its cross-talk with integrins, providing a basis for control of cell motility through glycosynapse. *J Biol Chem* 282(11): 8123–8133.
6. Saito T, Hakomori SI (1971) Quantitative isolation of total glycosphingolipids from animal cells. *J Lipid Res* 12(2):257–259.
7. Yu RK, Ledeen RW (1972) Gangliosides of human, bovine, and rabbit plasma. *J Lipid Res* 13(5):680–686.
8. Guan F, Handa K, Hakomori SI (2009) Specific glycosphingolipids mediate epithelial-to-mesenchymal transition of human and mouse epithelial cell lines. *Proc Natl Acad Sci USA* 106(18):7461–7466.

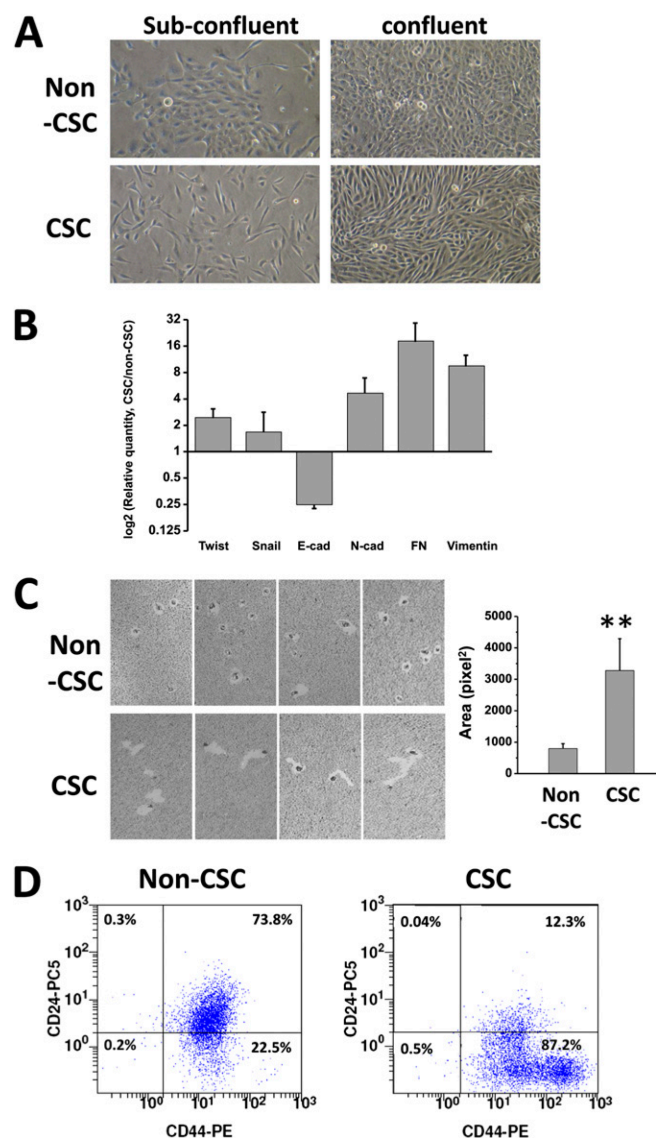

Fig. S1. EMT induction by expression of Twist-conferred cell with stem-cell properties. Induction of EMT by Twist expression in HMLE-Twist-ER cultured in the presence of tamoxifen for 12 d. HMLE-Twist-ER cells and Twist-expressing HMLE-Twist-ER cells were used as non-cancer stem cells (CSCs) and CSCs, respectively. (*A*) Phase-contrast images of the cells treated with tamoxifen for 12 d. (*B*) Expression levels of mRNAs encoding EMT-associated proteins in Twist-expressing HMLE-Twist-ER cells. β-Actin mRNA was used as reference gene to normalize. The data are shown as means ± SEM. (*C*) Cell motility was analyzed by gold colloidal phagokinetic track assay. Tracks from 30 individual cells were measured and quantified. Mean ± SD is shown. $^{**}P \leq 0.005$. (*D*) Expression profiles of CD24 and CD44 in non-CSCs and CSCs. Induction of EMT by Twist resulted in the appearance of $CD44^{hi}/CD24^{lo}$ cell populations.

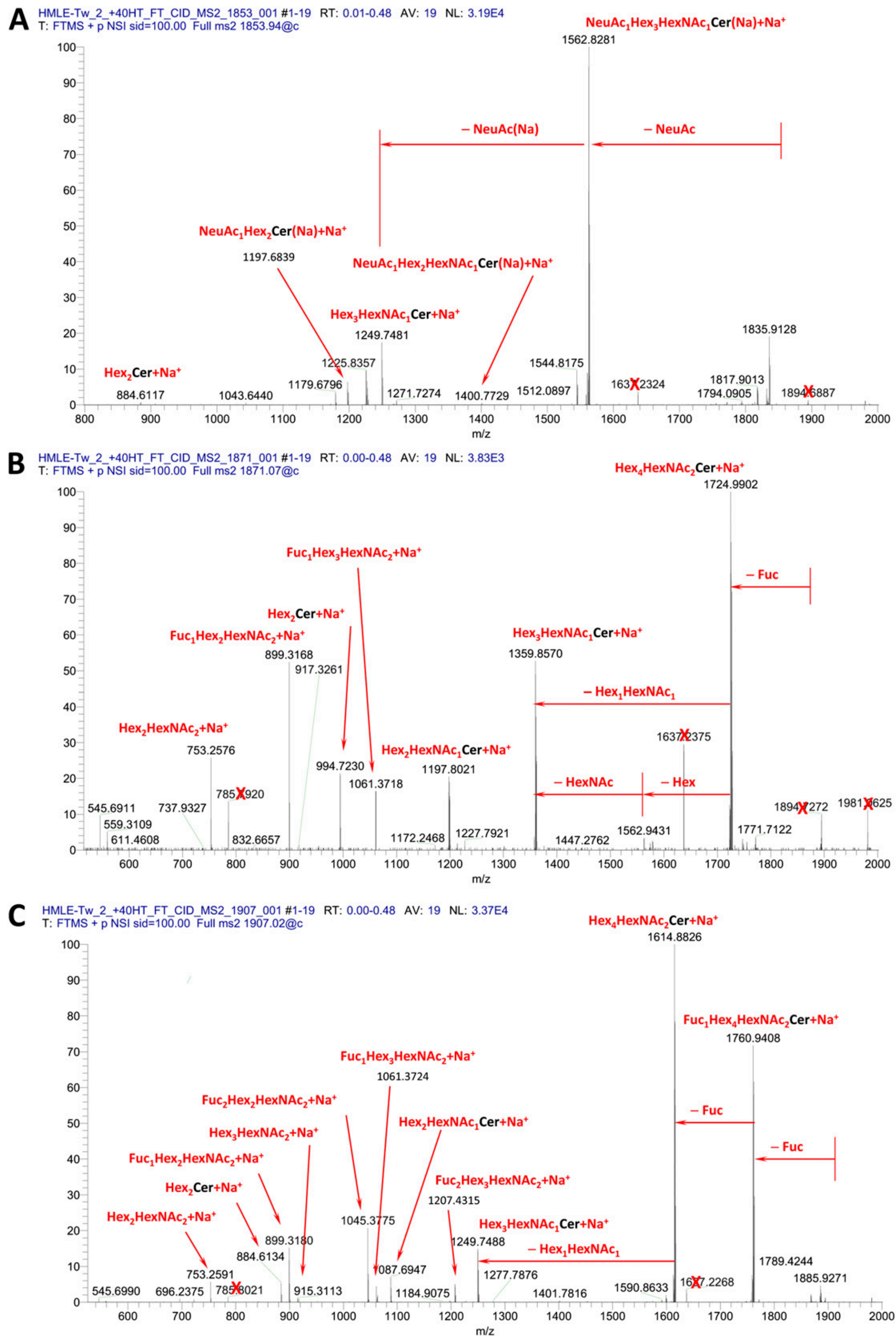

Fig. S2. Electrospray ionization–collision-induced dissociation–Fourier transform–MS2 (ESI-CID-FT-MS2) spectra of selected GSL molecular precursors from a CSC sample. (*A*) ESI-CID-FT-MS2 of precursor at *m/z* 1,853.94 corresponding to NeuAc2-Gg4Cer(Na)+Na^+ (Cer = d18:1/16:0) from a Breast Cancer Surveillance Consortium (BCSC) sample. Note that Na refers to salt formation at one NeuAc residue (i.e., M − H + Na), $\Delta m/z$ +21.9819, in contrast to +Na^+, which refers to sodium salt adduction, $\Delta m/z$ +22.9892. Note also that the exclusive and abundant loss of NeuAc residues, and absence of loss of Hex residue (or $Hex_1HexNAc_1$), from the molecular precursor ion is suggestive of GD1a, rather than GD1b, ganglioside structure, although the evidence is not definitive under these conditions (NeuAc losses are highly favored anyway). (*B*) ESI-CID-FT-MS2 of precursor at *m/z* 1,871.07 corresponding to Fuc-(n)Lc6Cer+Na^+ (Cer = d18:1/24:1) from a BCSC sample. Note that the exclusive and abundant loss of a Fuc residue, and absence of losses of Hex residue (or $Hex_2HexNAc_1$), from the molecular precursor ion is

Legend continued on following page

suggestive of type-2 chain (nLc) core structure (Le^x), although the evidence is not definitive under these conditions. H blood group structures (having nonreducing terminal Fuc) are also consistent with the observed fragmentation. (*C*) ESI-CID-FT-MS2 of precursor at *m/z* 1,907.02 corresponding to Fuc2-(n)Lc6Cer+ Na^+ (Cer = d18:1/16:0) from a BCSC sample. Note that the exclusive and abundant loss of Fuc residues, and absence of losses of Hex residue (or Fuc_1Hex_{2-} $HexNAc_1$), from the molecular precursor ion is suggestive of type-2 chain (nLc) core structure (Le^x), although the evidence is not definitive under these conditions. H blood group structures (having nonreducing terminal Fuc) are also consistent with the observed fragmentation. In all three spectra, X refers to known FT artifact peaks, which should be disregarded.

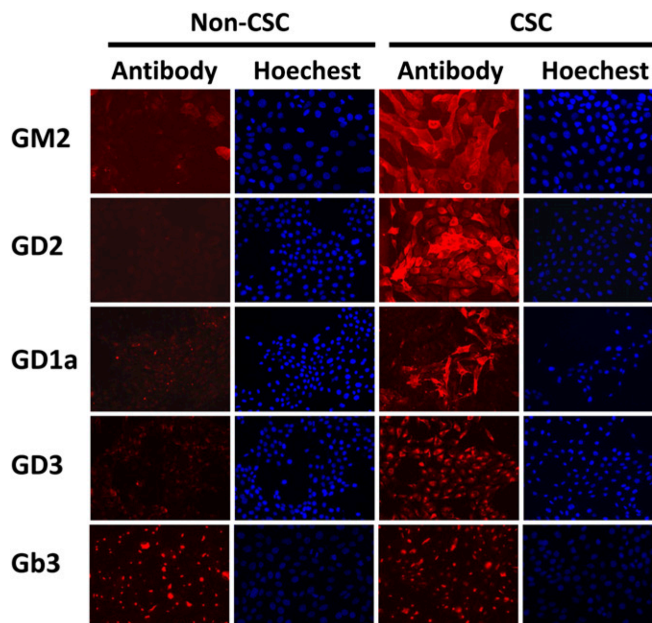

Fig. S3. Analysis of GSL expression by immunofluorescence cell staining. Semiconfluent monolayers of CSCs and non-CSCs were fixed and then stained with mAbs against each GSL as indicated. Appropriate secondary antibodies conjugated with Alexa Fluor 594 (red) were used. Hoechst staining (blue) was used for nuclei staining.

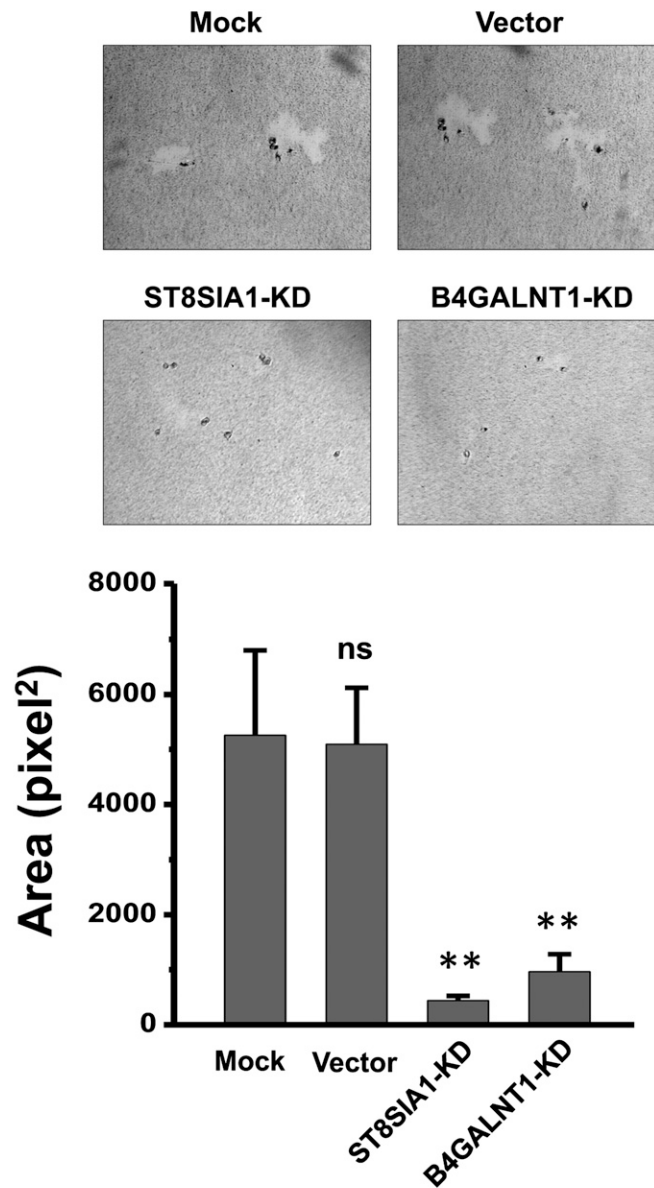

Fig. S4. Knockdown of ST8SIA1 and B4GALNT1 reduces cell motility in MCF-7 cells. ST8SIA1-KD or B4GALNT1-KD cells were incubated and grown for 18 h on gold sol-coated plates. The migrated area was measured as described in *Materials and Methods*. Data represent the mean of three independent experiments, $^{**}P \leq 0.005$.

Table S1. Generic structural formulae of GSLs detected in ESI-Orbitrap-MS1 of upper-phase fractions from cultured non-CSCs and CSCs

Input mass	Matched mass	Delta	Abbreviation	Z_0	Y_0	B_n	C_n	Formula	Ion
884.6207	884.6075	0.0132	Hex (2)-Cer(d18:1/16:0)	542.4913	560.5019	347.0954	365.106	C46H87NO13Na	[M+Na]+
968.7149	968.7014	0.0135	Hex (2)-Cer(d18:1/22:0)	626.5852	644.5958	347.0954	365.106	C52H99NO13Na	[M+Na]+
994.7322	994.7171	0.0151	Hex (2)-Cer(d18:1/24:1)	652.6008	670.6114	347.0954	365.106	C54H101NO13Na	[M+Na]+
1,046.6773	1,046.6603	0.017	Hex (3)-Cer(d18:1/16:0)	542.4913	560.5019	509.1482	527.1588	C52H97NO18Na	[M+Na]+
1,087.7049	1,087.6869	0.018	Hex (2)-HexNAc-Cer(d18:1/16:0)	542.4913	560.5019	550.1748	568.1854	C54H100N2O18Na	[M+Na]+
1,197.8136	1,197.7964	0.0172	Hex (2)-HexNAc-Cer(d18:1/24:1)	652.6008	670.6114	550.1748	568.1854	C62H114N2O18Na	[M+Na]+
1,175.723	1,175.7029	0.0201	Hex (2)-NeuAc-Cer(d18:1/16:0)	542.4913	560.5019	638.1908	656.2014	C57H104N2O21Na	[M+Na]+
1,257.8019	1,257.7812	0.0207	Hex (2)-NeuAc-Cer(d18:1/22:1)	624.5695	642.5801	638.1908	656.2014	C63H114N2O21Na	[M+Na]+
1,259.8164	1,259.7968	0.0196	Hex (2)-NeuAc-Cer(d18:1/22:0)	626.5852	644.5958	638.1908	656.2014	C63H116N2O21Na	[M+Na]+
1,285.8335	1,285.8125	0.021	Hex (2)-NeuAc-Cer(d18:1/24:1)	652.6008	670.6114	638.1908	656.2014	C65H118N2O21Na	[M+Na]+
1,287.8458	1,287.8281	0.0177	Hex (2)-NeuAc-Cer(d18:1/24:0)	654.6165	672.6271	638.1908	656.2014	C65H120N2O21Na	[M+Na]+
1,197.7063	1,197.6848	0.0215	Hex (2)-NeuAc-Cer(d18:1/16:0)	542.4913	560.5019	660.1727	678.1833	C57H103N2O21Na2	[M-H+2Na]+
1,279.7856	1,279.7631	0.0225	Hex (2)-NeuAc-Cer(d18:1/22:1)	624.5695	642.5801	660.1727	678.1833	C63H113N2O21Na2	[M-H+2Na]+
1,281.8	1,281.7787	0.0213	Hex (2)-NeuAc-Cer(d18:1/22:0)	626.5852	644.5958	660.1727	678.1833	C63H115N2O21Na2	[M-H+2Na]+
1,307.8169	1,307.7944	0.0225	Hex (2)-NeuAc-Cer(d18:1/24:1)	652.6008	670.6114	660.1727	678.1833	C65H117N2O21Na2	[M-H+2Na]+
1,309.8289	1,309.81	0.0189	Hex (2)-NeuAc-Cer(d18:1/24:0)	654.6165	672.6271	660.1727	678.1833	C65H119N2O21Na2	[M-H+2Na]+
1,249.7612	1,249.7397	0.0215	Hex (3)-HexNAc-Cer(d18:1/16:0)	542.4913	560.5019	712.2276	730.2382	C60H110N2O23Na	[M+Na]+
1,331.8409	1,331.818	0.0229	Hex (3)-HexNAc-Cer(d18:1/22:1)	624.5695	642.5801	712.2276	730.2382	C66H120N2O23Na	[M+Na]+
1,333.8546	1,333.8336	0.021	Hex (3)-HexNAc-Cer(d18:1/22:0)	626.5852	644.5958	712.2276	730.2382	C66H122N2O23Na	[M+Na]+
1,359.8711	1,359.8493	0.0218	Hex (3)-HexNAc-Cer(d18:1/24:1)	652.6008	670.6114	712.2276	730.2382	C68H124N2O23Na	[M+Na]+
1,395.8238	1,395.7976	0.0262	Hex (3)-HexNAc-Fuc-Cer(d18:1/16:0)	542.4913	560.5019	858.2855	876.2961	C66H120N2O27Na	[M+Na]+
1,505.9346	1,505.9072	0.0274	Hex (3)-HexNAc-Fuc-Cer(d18:1/24:1)	652.6008	670.6114	858.2855	876.2961	C74H134N2O27Na	[M+Na]+
1,541.8709	1,541.8555	0.0154	Hex (3)-HexNAc-Fuc (2)-Cer(d18:1/16:0)	542.4913	560.5019	1,004.3434	1,022.354	C72H130N2O31Na	[M+Na]+
1,378.8068	1,378.7823	0.0245	Hex (2)-HexNAc-NeuAc-Cer(d18:1/16:0)	542.4913	560.5019	841.2702	859.2808	C65H117N3O26Na	[M+Na]+
1,460.8865	1,460.8606	0.0259	Hex (2)-HexNAc-NeuAc-Cer(d18:1/22:1)	624.5695	642.5801	841.2702	859.2808	C71H127N3O26Na	[M+Na]+
1,462.8991	1,462.8762	0.0229	Hex (2)-HexNAc-NeuAc-Cer(d18:1/22:0)	626.5852	644.5958	841.2702	859.2808	C71H129N3O26Na	[M+Na]+
1,488.9173	1,488.8919	0.0254	Hex (2)-HexNAc-NeuAc-Cer(d18:1/24:1)	652.6008	670.6114	841.2702	859.2808	C73H131N3O26Na	[M+Na]+
1,490.9285	1,490.9075	0.021	Hex (2)-HexNAc-NeuAc-Cer(d18:1/24:0)	654.6165	672.6271	841.2702	859.2808	C73H133N3O26Na	[M+Na]+
1,400.7898	1,400.7642	0.0256	Hex (2)-HexNAc-NeuAc-Cer(d18:1/16:0)	542.4913	560.5019	863.2521	881.2627	C65H116N3O26Na2	[M-H+2Na]+
1,510.8986	1,510.8738	0.0248	Hex (2)-HexNAc-NeuAc-Cer(d18:1/24:1)	652.6008	670.6114	863.2521	881.2627	C73H130N3O26Na2	[M-H+2Na]+
1,512.9104	1,512.8894	0.021	Hex (2)-HexNAc-NeuAc-Cer(d18:1/24:0)	654.6165	672.6271	863.2521	881.2627	C73H132N3O26Na2	[M-H+2Na]+
1,540.8631	1,540.8351	0.028	Hex (3)-HexNAc-NeuAc-Cer(d18:1/16:0)	542.4913	560.5019	1,003.323	1,021.3336	C71H127N3O31Na	[M+Na]+
1,622.9406	1,622.9134	0.0272	Hex (3)-HexNAc-NeuAc-Cer(d18:1/22:1)	624.5695	642.5801	1,003.323	1,021.3336	C77H137N3O31Na	[M+Na]+
1,624.9564	1,624.929	0.0274	Hex (3)-HexNAc-NeuAc-Cer(d18:1/22:0)	626.5852	644.5958	1,003.323	1,021.3336	C77H139N3O31Na	[M+Na]+
1,650.973	1,650.9447	0.0283	Hex (3)-HexNAc-NeuAc-Cer(d18:1/24:1)	652.6008	670.6114	1,003.323	1,021.3336	C79H141N3O31Na	[M+Na]+
1,652.9852	1,652.9603	0.0249	Hex (3)-HexNAc-NeuAc-Cer(d18:1/24:0)	654.6165	672.6271	1,003.323	1,021.3336	C79H143N3O31Na	[M+Na]+
1,562.8454	1,562.817	0.0284	Hex (3)-HexNAc-NeuAc-Cer(d18:1/16:0)	542.4913	560.5019	1,025.3049	1,043.3155	C71H126N3O31Na2	[M-H+2Na]+
1,644.9227	1,644.8953	0.0274	Hex (3)-HexNAc-NeuAc-Cer(d18:1/22:1)	624.5695	642.5801	1,025.3049	1,043.3155	C77H136N3O31Na2	[M-H+2Na]+
1,646.9377	1,646.9109	0.0268	Hex (3)-HexNAc-NeuAc-Cer(d18:1/22:0)	626.5852	644.5958	1,025.3049	1,043.3155	C77H138N3O31Na2	[M-H+2Na]+
1,672.9545	1,672.9266	0.0279	Hex (3)-HexNAc-NeuAc-Cer(d18:1/24:1)	652.6008	670.6114	1,025.3049	1,043.3155	C79H140N3O31Na2	[M-H+2Na]+
1,674.9667	1,674.9422	0.0245	Hex (3)-HexNAc-NeuAc-Cer(d18:1/24:0)	654.6165	672.6271	1,025.3049	1,043.3155	C79H142N3O31Na2	[M-H+2Na]+
1,614.9016	1,614.8719	0.0297	Hex (4)-HexNAc (2)-Cer(d18:1/16:0)	542.4913	560.5019	1,077.3598	1,095.3704	C74H133N3O33Na	[M+Na]+
1,725.009	1,724.9815	0.0275	Hex (4)-HexNAc (2)-Cer(d18:1/24:1)	652.6008	670.6114	1,077.3598	1,095.3704	C82H147N3O33Na	[M+Na]+
1,760.9591	1,760.9298	0.0293	Hex (4)-HexNAc (2)-Fuc-Cer(d18:1/16:0)	542.4913	560.5019	1,223.4177	1,241.4283	C80H143N3O37Na	[M+Na]+
1,843.0398	1,843.0081	0.0317	Hex (4)-HexNAc (2)-Fuc-Cer(d18:1/22:1)	624.5695	642.5801	1,223.4177	1,241.4283	C86H153N3O37Na	[M+Na]+
1,845.0538	1,845.0237	0.0301	Hex (4)-HexNAc (2)-Fuc-Cer(d18:1/22:0)	626.5852	644.5958	1,223.4177	1,241.4283	C86H155N3O37Na	[M+Na]+

Table S1. Cont.

Input mass	Matched mass	Delta	Abbreviation	Z_0	Y_0	B_n	C_n	Formula	Ion
1,871.0707	1,871.0394	0.0313	Hex (4)-HexNAc (2)-Fuc-Cer(d18:1/24:1)	652.6008	670.6114	1,223.4177	1,241.4283	C88H157N3O37Na	[M+Na]+
1,873.0805	1,873.055	0.0255	Hex (4)-HexNAc (2)-Fuc-Cer(d18:1/24:0)	654.6165	672.6271	1,223.4177	1,241.4283	C88H159N3O37Na	[M+Na]+
1,907.0163	1,906.9877	0.0286	Hex (4)-HexNAc (2)-Fuc (2)-Cer(d18:1/16:0)	542.4913	560.5019	1,369.4756	1,387.4862	C86H153N3O41Na	[M+Na]+
1,991.1125	1,991.0816	0.0309	Hex (4)-HexNAc (2)-Fuc (2)-Cer(d18:1/22:0)	626.5852	644.5958	1,369.4756	1,387.4862	C92H165N3O41Na	[M+Na]+
2,017.1261	2,017.0973	0.0288	Hex (4)-HexNAc (2)-Fuc (2)-Cer(d18:1/24:1)	652.6008	670.6114	1,369.4756	1,387.4862	C94H167N3O41Na	[M+Na]+
2,019.1369	2,019.1129	0.024	Hex (4)-HexNAc (2)-Fuc (2)-Cer(d18:1/24:0)	654.6165	672.6271	1,369.4756	1,387.4862	C94H169N3O41Na	[M+Na]+
1,466.8248	1,466.7984	0.0264	Hex (2)-NeuAc (2)-Cer(d18:1/16:0)	542.4913	560.5019	929.2863	947.2968	C68H121N3O29Na	[M+Na]+
1,576.9355	1,576.9079	0.0276	Hex (2)-NeuAc (2)-Cer(d18:1/24:1)	652.6008	670.6114	929.2863	947.2968	C76H135N3O29Na	[M+Na]+
1,578.9482	1,578.9236	0.0246	Hex (2)-NeuAc (2)-Cer(d18:1/24:0)	654.6165	672.6271	929.2863	947.2968	C76H137N3O29Na	[M+Na]+
1,669.8994	1,669.8777	0.0217	Hex (2)-HexNAc-NeuAc (2)-Cer(d18:1/16:0)	542.4913	560.5019	1,132.3656	1,150.3762	C76H134N4O34Na	[M+Na]+
1,780.0188	1,779.9873	0.0315	Hex (2)-HexNAc-NeuAc (2)-Cer(d18:1/24:1)	652.6008	670.6114	1,132.3656	1,150.3762	C84H148N4O34Na	[M+Na]+
1,782.0291	1,782.0029	0.0262	Hex (2)-HexNAc-NeuAc (2)-Cer(d18:1/24:0)	654.6165	672.6271	1,132.3656	1,150.3762	C84H150N4O34Na	[M+Na]+
1,831.9613	1,831.9306	0.0307	Hex (3)-HexNAc-NeuAc (2)-Cer(d18:1/16:0)	542.4913	560.5019	1,294.4185	1,312.429	C82H144N4O39Na	[M+Na]+
1,916.0544	1,916.0245	0.0299	Hex (3)-HexNAc-NeuAc (2)-Cer(d18:1/22:0)	626.5852	644.5958	1,294.4185	1,312.429	C88H156N4O39Na	[M+Na]+
1,942.0723	1,942.0401	0.0322	Hex (3)-HexNAc-NeuAc (2)-Cer(d18:1/24:1)	652.6008	670.6114	1,294.4185	1,312.429	C90H158N4O39Na	[M+Na]+
1,944.0834	1,944.0558	0.0276	Hex (3)-HexNAc-NeuAc (2)-Cer(d18:1/24:0)	654.6165	672.6271	1,294.4185	1,312.429	C90H160N4O39Na	[M+Na]+
1,853.9431	1,853.9125	0.0306	Hex (3)-HexNAc-NeuAc (2)-Cer(d18:1/16:0)	542.4913	560.5019	1,316.4004	1,334.4109	C82H141N4O39Na2	[M-H+2Na]+
1,938.0377	1,938.0064	0.0313	Hex (3)-HexNAc-NeuAc (2)-Cer(d18:1/22:0)	626.5852	644.5958	1,316.4004	1,334.4109	C88H155N4O39Na2	[M-H+2Na]+
1,964.0532	1,964.022	0.0312	Hex (3)-HexNAc-NeuAc (2)-Cer(d18:1/24:1)	652.6008	670.6114	1,316.4004	1,334.4109	C90H157N4O39Na2	[M-H+2Na]+
1,966.0643	1,966.0377	0.0266	Hex (3)-HexNAc-NeuAc (2)-Cer(d18:1/24:0)	654.6165	672.6271	1,316.4004	1,334.4109	C90H159N4O39Na2	[M-H+2Na]+
1,875.925	1,875.8944	0.0306	Hex (3)-HexNAc-NeuAc (2)-Cer(d18:1/16:0)	542.4913	560.5019	1,338.3823	1,356.3928	C82H142N4O39Na3	[M-2H+3Na]+
1,960.0183	1,959.9883	0.03	Hex (3)-HexNAc-NeuAc (2)-Cer(d18:1/22:0)	626.5852	644.5958	1,338.3823	1,356.3928	C88H154N4O39Na3	[M-2H+3Na]+
1,986.0325	1986.0039	0.0286	Hex (3)-HexNAc-NeuAc (2)-Cer(d18:1/24:1)	652.6008	670.6114	1,338.3823	1,356.3928	C90H156N4O39Na3	[M-2H+3Na]+
1,988.0461	1,988.0196	0.0265	Hex (3)-HexNAc-NeuAc (2)-Cer(d18:1/24:0)	654.6165	672.6271	1,338.3823	1,356.3928	C90H158N4O39Na3	[M-2H+3Na]+

Fragment ion nomenclature according to Domon and Costello (1). Y_0 and Z_0 represent ceramide ions respectively including and excluding the glycosidic oxygen atom (differing by 18 due to differential proton transfers accompanying fragmentation). C_n and B_n represent whole glycan ions respectively including and excluding the glycosidic oxygen atom (also differing by 18 due to differential proton transfers accompanying fragmentation). All mass numbers (columns 1, 2 , 5, 6, 7, and 8) are given in units of m/z (mass-to-charge ratio).

1. Domon B, Costello CE (1988) A systematic nomenclature for carbohydrate fragmentations in FAB–MS/MS spectra of glycoconjugates. *Glycoconj J* 5:397–409.